Journal of Fluids and Structures 17 (2003) 915–926

JOURNAL OF FLUIDS AND STRUCTURES

www.elsevier.nl/locate/jnlabr/yjfls

Spring stiffness influence on an oscillating propulsor

M.M. Murray[a], L.E. Howle[b,c,*]

[a] Department of Mechanical Engineering, United States Naval Academy, Annapolis, MD 21403, USA
[b] Department of Mechanical Engineering and Materials Science, Duke University, Durham, NC 27708-0300, USA
[c] Center for Nonlinear and Complex Systems, Duke University, Durham, NC 27708-0300, USA

Received 17 July 2000; accepted 22 February 2003

Abstract

We study the propulsive dynamics of a thin foil pitching about its quarter chord and allowed to passively plunge. Specifically, we focus on the effect of variations in translational spring stiffness on propulsor plunge and on the minimum oscillation frequency required to produce positive thrust. Our numerical simulation utilizes a two-dimensional hydroelasticity model of the propulsor–fluid system in a constant velocity free stream. The pitch is forced at the quarter chord by a drive shaft and the dynamics of the fluid–structure interaction coupled to the strength of a translational spring determines the plunge amplitude. We use an unsteady two-dimensional vortex lattice method to model the hydrodynamics of the propulsor producing thrust in a potential flow field. The phase relationship between the driving angle and the plunge displacement is discussed, along with the effects of changing spring stiffness on thrust and efficiency. We show that passive plunge reduces the critical frequency for positive thrust production. This allows simple one-actuator input to compete with more complicated two-actuator systems.
© 2003 Elsevier Ltd. All rights reserved.

1. Introduction

The subject of using an oscillatory motion to produce thrust has been analyzed for many years in the context of swimming fish (Breder, 1926; Gray, 1936; Marey, 1874; Pettigrew, 1874; Taylor, 1952). There has been a considerable effort made to mimic the propulsive dynamics of aquatic animals. In fact there have been a number of efforts made to construct machines which utilize oscillatory motion to produce propulsive thrust (Triantafyllou and Triantafyllou, 1995; Anderson and Kerrebrock, 1999; Kumph et al., 1999). Most of these efforts resulted in complex mechanical systems utilizing hydraulic or pneumatic power systems. While the design and successful manufacture of a man-made aquatic swimming device is of interest to engineers and biologists, the challenges posed by such a device are large. An alternative approach, one we employ, is the use of simplified devices for thrust production.

Several investigators utilize simplified models of the complex motion of aquatic animals to obtain a better understanding of the structural motions required to produce thrust (Lighthill, 1960; Saffman, 1967; Wu, 1961). An oscillating airfoil is one commonly used simplified model for studying aquatic thrust production. Garrick (1937) utilized the formulas developed by Theodorsen (1935) for a flat plate oscillating in potential flow and the methods outlined by von Kármán and Burgers (1935) to obtain formulas for the thrust and efficiency of a pitching and plunging airfoil. Garrick showed analytically that for pure plunging motion all frequencies of oscillation produce positive thrust, and for pure pitching motion, the oscillation frequency must be greater than a critical value in order to produce positive thrust. Chopra (1974) studied the utility of a plate undergoing small amplitude pitching and plunging to model the thrust and

*Corresponding author. Department of Mechanical Engineering and Materials Science, Duke University, P.O. Box 90300, Hudson Hall 225, Hudson Engineering Centre, Durham, NC 27708, USA. Tel.: +1-919-660-5310; fax: +1-919-660-8963.
E-mail address: laurens.howle@duke.edu (L.E. Howle).

0889-9746/03/$ - see front matter © 2003 Elsevier Ltd. All rights reserved.
doi:10.1016/S0889-9746(03)00026-4

efficiency of tail fins of aquatic animals. Chopra later developed a two-dimensional model not dependent on small amplitudes (Chopra, 1976), and also a model for a finite flat-plate wing of general planform (Chopra and Kambe, 1977). He showed that high efficiencies are possible for various combinations of pitch and plunge. Our approach takes advantage of this combination of pitching and plunging motion to achieve high efficiencies without requiring direct translational actuation.

Delaurier and Harris (1982) performed low-speed wind tunnel experiments of thrust production by an airfoil plunging sinusoidally with superimposed pitching of variable amplitude and phase. Although the experimental system introduced some inaccuracies due to inertial forces, they found that the best thrust performance occurred at phase angles of 90–120° with pitch lagging plunge. It was further shown that the highest thrust values were obtained with maximum pitching amplitudes of 12.5°. Triantafyllou et al. (1991, 1993) performed experiments and analysis of a heaving and pitching airfoil producing thrust at a fixed pitch/plunge phase angle of 90°. The maximum efficiency occurred in a nondimensional frequency that corresponds to the tail beat frequency of many common fishes; a Strouhal number of 0.25–0.35. Anderson et al. (1998) performed an experimental study of thrust production and efficiency of a foil sinusoidally plunging and pitching at a variety of angles, pitch/plunge phase, and pitch/plunge relative amplitude. Force, power, and flow visualization data were employed to help analyze the results. Efficiencies as high as 87% are found for plunge/pitch combinations that produce a leading edge vortex that interacts with the trailing edge of the foil. Optimal thrust was produced at Strouhal number 0.25–0.4. Harper et al. (1998) modelled an oscillating foil producing thrust where the heaving and pitching actuators are attached to the foil by springs. Simplified analytic expressions derived from Theodorsen's work (1935) are utilized to describe the hydrodynamic forces, and are coupled with rigid body mechanics equations to analyze dynamics of differing spring stiffness values. It was shown that optimal spring values can reduce the energy required for actuation. Our analysis uses the similar concept of utilizing springs to alter the foil dynamics, but with fundamental differences. The analysis of Harper et al. (1998) requires both translational and rotational actuation and seeks to obtain optimal efficiency for specific actuation parameters by optimizing spring design. Our analysis seeks to obtain the higher efficiency benefits associated with pitch and plunge motion, through the passive plunging dynamics associated with a foil supported by a translational spring and driven by a single rotational actuator.

Analysis of the vortical wake structure shed from a moving surface reveals qualitative and quantitative information about the forces generated by the surface. von Kármán and Burgers (1935) explained the ability of an oscillating airfoil to produce thrust by considering the relative orientation and rotational direction of vorticity shed into the wake. A qualitative analysis of the velocity field produced by the wake vorticity demonstrates that an impulse is imparted to the fluid in the form of fluid jets. The impulse imparted to the fluid is in reaction to the positive thrust force produced by the airfoil. Jones et al. (1998) performed a detailed investigation of the vortical structures formed in the wake of a plunging airfoil using both experimental methods and numerical simulations. A key finding of their work was that wake asymmetries can exist for large Strouhal numbers, probably due to viscous effects such as flow separation. Koochesfahani (1989) performed an experimental examination of vortical flow patterns of a small-amplitude thrust-producing pitching airfoil in a low speed water channel, and found that the structure of the wake can be substantially changed by the amplitude, frequency and waveform of oscillation. Koochesfahani found, by analysis of the mean wake velocity, that the critical frequency for thrust production is higher than that calculated by linear theory and is dependent on oscillating amplitude. This is due to the additional thrust needed to overcome viscous drag in a real fluid. Katz and Weihs (1981) showed that wake roll-up calculations utilizing the trailing-edge Kutta condition for oscillating propulsors were in good agreement flow visualization data over a large range of frequencies. They concluded that the Kutta condition can be applied for oscillations with small trailing edge amplitudes in force and moment predictions to a reduced frequency of approximately 1.0. This is not the case for large-amplitude motion because flow separation invalidates the trailing edge Kutta condition. Hall et al. (1997) used variational methods to describe the minimum power requirements required for flapping flight. The optimal circulation distribution required to simultaneously generate thrust and lift are given. A detailed explanation of the effects that could cause a difference between experimental observations and calculated values were also given. Hall and Hall (1996) showed that the optimal distribution of shed vorticity places most of vorticity at the extremes of the trailing edge flight path with a rotational sense that produces a jet in the direction opposite that of thrust generation. In our work we qualitatively analyze wake structure to help identify the dynamics associated with high efficiency response.

In this work, we examine the problem of thrust generation by a simply actuated foil. In analyzing the propulsive utility of an oscillating foil, we shall keep in mind the following key points—gleaned from the aforementioned studies: (i) plunging foils in a potential flow produce thrust for any frequency; (ii) pitching foils must exceed a critical frequency before producing thrust; (iii) a plunging foil is generally more efficient than a pitching foil; (iv) the optimal combination of pitch and plunging places most of the shed vorticity at the extremes of the trailing-edge path so that the resulting wake structure convects fluid away from the foil.

It is evident from the first three of these points that an efficient foil propulsor should have double actuation; both pitch and plunge, although at least one highly maneuverable unmanned underwater vehicle uses only pitching actuation (Hobson et al., 1999). Rather than study this general problem, our goal is to analyze a single actuated degree of freedom with the second degree of freedom passively determined by the system dynamics. More precisely, we study a simple model of a stiff propulsor oscillating about the quarter chord, with the pivot point attached to a linear translational spring. The spring allows the propulsor to plunge in proportion to the lifting force. This system recovers the benefits [points (i)–(iv), above] of doubly actuated foil propulsors but at a simplified mechanical cost.

2. Numerical model

We assume that the fluid field of interest is incompressible, inviscid, and irrotational. The fluid field can therefore be described using a potential flow model with the equation describing the flow field being

$$\nabla^2 \Phi = 0, \tag{1}$$

where Φ is the velocity potential. With an object submerged in a free stream of constant velocity and utilizing linear theory, the momentum equation becomes

$$\frac{p_\infty - p}{\rho} \approx U_\infty \frac{\partial \Phi}{\partial x} + \frac{\partial \Phi}{\partial t}, \tag{2}$$

where p_∞ is the pressure of the freestream, p is the local pressure, ρ is the fluid density, and U_∞ is the freestream velocity. In determining the dynamics of the propulsor, it is important to obtain the difference in pressure between the bottom and top of the propulsor. The pressure difference is described utilizing the vortex distribution on the propulsor and is

$$\Delta p(x) = \rho \left[U_\infty \gamma(x,t) + \frac{\partial}{\partial t} \int_0^x \gamma(x_0,t)\, \mathrm{d}x_0 \right], \tag{3}$$

where $\Delta p(x)$ is the pressure difference between the upper and lower surfaces of the propulsor, and $\gamma(x,t)$ is the vortex distribution on the propulsor.

We use an unsteady two-dimensional vortex lattice technique to model the hydrodynamic portion of the problem. The propulsor pivot point is allowed to translate perpendicularly to the flow in response to the instantaneous hydrodynamic forces placed on the foil by the fluid. This motion is resisted by a translational spring attached at the pivot location, the quarter chord of the foil, as shown in Fig. 1. By allowing the structure to fluid density ratio to approach unity and considering a thin propulsor, it is assumed that inertial effects of the propulsor mass are negligible, and the system inertial effects are dominated by the 'added mass' of the fluid. We have considered the effects of linear and rotational inertia of the foil elsewhere (Murray, 1999) and found that the dynamics were not significantly altered for thin foil cases of reasonable density. With the mass of the propulsor neglected, the deflection of the translational spring is calculated directly from the sum of the hydrodynamic lifting forces on the propulsor. Therefore, the equation that describes the translational spring model is

$$h = \frac{\int_0^c \Delta p(x)\, \mathrm{d}x}{K}, \tag{4}$$

where h is the translational displacement of the quarter chord pivot point, K is the translational spring constant in units of force/displacement per unit span, and $\Delta p(x)$ is calculated using Eq. (3).

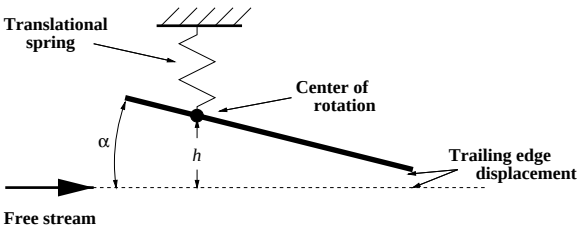

Fig. 1. Model of an oscillating zero-thickness foil. The propulsor is actuated in the pitching direction. The pitch pivot is constrained to move in the vertical direction. A linear spring connects the pivot to the translation coordinate system. Deviation of the pivot from the unstrained position is through forces exerted on the propulsor by the fluid.

In using an unsteady two-dimensional vortex lattice technique to model the hydrodynamic portion of the problem, the wash normal to the propulsor surface is required. With the propulsor's ability to translate and utilizing a small angle approximation, the equation that represents the normal wash term becomes

$$w(x) = \dot{h} - U_\infty \alpha - \dot{\alpha} x_p, \tag{5}$$

where $w(x)$ is the normal wash, $\dot{h}$ is the pivot point velocity in the perpendicular displacement direction, α is the angle of attack, $\dot{\alpha}$ is the angular velocity, and x_p is the signed position from the pivot point.

For the unsteady time-dependent coupled system, the total solution is solved implicitly at each time step, with the vortex distribution and spring response solved simultaneously. The solution of these equations at each time step produces the values for pivot point deflection and vorticity along the propulsor. These values allow the calculation of vorticity shed into the wake and the lift on the propulsor. The boundary condition (5) introduces time-dependence into the potential flow problem (1) that, otherwise, appears to be independent of time. The boundaries of this potential flow model consist of the foil surface and the wake sheet.[1]

The Kelvin circulation theorem specifies the strength of the vorticity that is shed into the wake. Kelvin's circulation theorem states that, for an incompressible, inviscid flow, the time rate of change of circulation around a given set of fluid particles is zero and is written as

$$\frac{D\Gamma}{Dt} = 0, \tag{6}$$

where Γ is the total (foil plus wake) circulation. We use Eq. (6) to calculate the strength of the vortex element that is shed from the trailing edge of the propulsor at each time step by equating to zero the difference between the total circulation just prior to and just after the vortex element is shed. Thus, the discrete version of Eq. (6), which specifies the shed vortex strength,[2] is

$$\Gamma_{\text{shed}} = \sum_{j=1}^{N} (\Gamma_j^{n+1} - \Gamma_j^n), \tag{7}$$

where Γ_{shed} is the strength of the shed vortex. Γ_j^n and Γ_j^{n+1} are the strengths of individual propulsor vortex elements at the previous and current time step, respectively. N is the total number of panels which make up the propulsor. We determine Γ_{shed} at each time step simultaneously with center-line deflection and foil vortex strength distribution.

The calculation of thrust and efficiency, given in the following section, requires the analysis of the vortex sheet shed into the wake. The accurate calculation of vortex sheet evolution in the wake is difficult because the singular nature of the Birkhoff–Rott kernel makes the problem linearly ill-posed. Desingularization of the kernel is required for useful information to be obtained. The reader is directed to a work by Krasny (1987). The influence of wake roll-up near the foil was shown to have negligible effects on the circulation distribution for practical frequencies and numerical studies show that this is the case for even large-amplitude flapping motions with large hydrodynamic loads (Hall and Hall, 2000). Therefore, our thrust and efficiency calculations utilize a fixed wake model.

2.1. Thrust and efficiency calculations

Our calculations of average propulsor thrust and efficiency are not standard for vortex lattice methods, we will therefore derive them in more detail than the previous quantities. The vortex lattice model can directly calculate thrust, but it has to be done carefully. The difficulty in accurately calculating the thrust produced by the propulsor comes from correctly determining the contribution of the 'leading edge suction' of the propulsor (Katz and Plotkin, 2001). This term is a direct consequence of the $1/\sqrt{x}$ behavior of the vorticity distribution on a flat plate at the leading edge. An analytical approach can be utilized to calculate the thrust produced by a flat plate (Garrick, 1937; Harper et al., 1998). An alternate method, suggested by Hall and Hall (1996), and used in this work, utilizes the concept of Kelvin impulse to calculate the time-averaged thrust from the wake produced by the propulsor. The thrust and lift on the propulsor are a direct consequence of the increase in momentum of the fluid surrounding the body.

We assume that the propulsor oscillates periodically, and has been oscillating for a sufficiently long time that the wake effects on the propulsor are periodic. Therefore, the change in momentum of the fluid over one period of flapping can be calculated from the momentum contained in the wake over one period.

[1] The wake sheet is considered a kinematic material boundary for time-dependent two-dimensional vortex lattice models, see Katz and Plotkin (2001).

[2] For zero initial circulation.

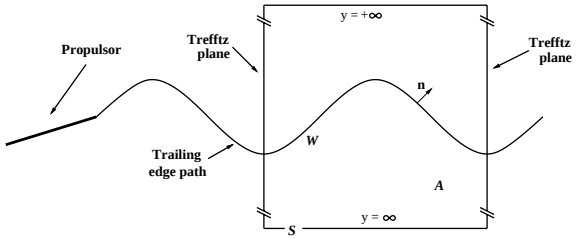

Fig. 2. Trefftz volume used to compute the Kelvin impulse in the periodic wake. From this quantity, we compute the cycle-averaged thrust.

To calculate the average momentum deposited in the wake over one period, we utilize a Trefftz volume, as shown in Fig. 2. We choose a two-dimensional 'volume' so that the upper and lower boundaries are at infinity, and the vertical boundaries are set one period apart, or a distance of UT (where T is the period of flapping). The Kelvin impulse $\boldsymbol{\xi}$ is

$$\boldsymbol{\xi} = \rho \int \int_A \nabla\phi \, \mathrm{d}A, \tag{8}$$

with ϕ the velocity potential and the integral is taken over A, which is the area bounded by the Trefftz planes. The reader is referred to Ashley and Landahl (1965) for further detail of thrust calculation in the Trefftz volume. We use Gauss' theorem to transfer the integral from the two-dimensional 'volume' to the boundaries. Eq. (8) becomes

$$\boldsymbol{\xi} = -\rho \int_S \phi \mathbf{n} \, \mathrm{d}S, \tag{9}$$

where $\mathbf{n}$ is the unit normal pointing into the fluid. The construction of the Trefftz volume allows us to assume that the contribution from the upper and lower boundaries at infinity are zero because the disturbance is vanishingly small far from the body. The contributions from the two vertical planes cancel due to the assumption of periodicity, with the normal vectors pointing in opposite directions. Therefore the integral of Eq. (9) is taken over only the top and bottom of the wake. Eq. (9) then becomes

$$\boldsymbol{\xi} = -\rho \int_W (\phi_u - \phi_l)\mathbf{n} \, \mathrm{d}S = -\rho \int_W \Gamma \mathbf{n} \, \mathrm{d}S, \tag{10}$$

where $\phi_u - \phi_l$ represents the difference in velocity potential when the integral is taken over the upper and lower faces of the wake. Γ is the circulation associated with the wake vortex sheet.

The average force imparted onto the thruster is simply the negative of the impulse imparted into the fluid divided by the time it takes to impart the impulse. Therefore,

$$\mathbf{F} = -\frac{\boldsymbol{\xi}}{T} = \frac{\rho}{T} \int_W \Gamma \mathbf{n} \, \mathrm{d}S, \tag{11}$$

where $\mathbf{F}$ is the time-averaged force and T is the period of oscillation. We obtained the time-averaged thrust by finding the x component of force, so

$$T_{\mathrm{ave}} = -\frac{\rho}{T} \int_W \Gamma \mathbf{n} \cdot \mathbf{i} \, \mathrm{d}S, \tag{12}$$

where T_{ave} is the average thrust produced by the oscillating propulsor in one period. The useful average power produced by the thruster is

$$P_{\mathrm{out}} = T_{\mathrm{ave}} U_\infty \tag{13}$$

which is simply the average thrust force multiplied by the velocity.

The instantaneous input power of the shaft can be calculated by analyzing the time-dependent torque on the shaft and multiplying by the time-dependent angular velocity. To obtain the average input power we use

$$P_{\mathrm{in}} = \frac{1}{T} \int_t^{t+T} \boldsymbol{\tau}_{\mathrm{s}} \cdot \boldsymbol{\omega}_{\mathrm{s}} \, \mathrm{d}t, \tag{14}$$

where $\boldsymbol{\tau}_{\mathrm{s}}$ is the torque produced by the shaft and $\boldsymbol{\omega}_{\mathrm{s}}$ is the angular velocity of the shaft. The torque is calculated by multiplying the lifting forces on each panel by their distance from the pivot point, and again assuming that the inertial effects of the zero thickness foil are negligible.

The efficiency is calculated simply as

$$\eta = \frac{P_{\text{out}}}{P_{\text{in}}}, \tag{15}$$

where Eq. (13) gives P_{out} and Eq. (14) gives P_{in}. It must be noted that this is a maximum value for efficiency, because the power loss incurred from viscous drag is not considered in our model.

2.2. Terminology

The discussion of our results requires that several normalized terms be defined. The first is the normalized frequency of foil oscillation

$$\text{St}_c = \frac{fc}{U_\infty}, \tag{16}$$

where St_c is the Strouhal number based on chord, f is the driving frequency, c is the chord length, and U_∞ is the free stream velocity. The pivot displacement (plunge) is normalized by the chord length

$$h' = \frac{h}{c}. \tag{17}$$

The thrust coefficient, C_T, is defined along the same lines as the coefficient of lift for an airfoil, and is

$$C_T = \frac{T_{\text{ave}}}{\frac{1}{2}\rho U_\infty^2 c}, \tag{18}$$

where T_{ave} is the average thrust per unit span and ρ is the density of the fluid. Although it is more common to normalize the Strouhal number and thrust coefficient by the trailing edge amplitude, we choose the chord because the trailing edge amplitude changes with different parameters examined in this study.

We also normalize the translational spring stiffness as

$$K_n = \frac{K}{\frac{1}{2}\rho U_\infty^2}, \tag{19}$$

where K is the spring constant given in units of force per displacement per unit span.

In order to confirm the validity of our numerical model, we compared the lift and moment responses to the analytical results originally derived by Theodorsen (1935) for a simplified problem. The numerical and analytical results were nearly identical. Further details of the validation of this numerical model may be found elsewhere (Murray, 1999).

3. Numerical results

In this section we demonstrate the effect that translational spring stiffness has on thrust, efficiency, and the minimum oscillation frequency required to produce positive thrust—the critical frequency. Following the discussion of the performance metrics, we explore the plunge amplitude of the pivot point, the trailing edge plunge amplitude, and the phase between the imposed pitch and the resulting plunge.

3.1. Critical frequency for thrust production

In discussing the critical frequency, we should also include discussions of purely pitching and purely plunging motions. When a flap plunges in an ideal fluid, it produces thrust for any frequency (Garrick, 1937). Conversely, a pitching flap produces thrust after the frequency exceeds a critical value (Garrick, 1937; Koochesfahani, 1989). For a given frequency, the optimal actuation schedule in terms of thrust contains both pitch and plunge (Dickinson et al., 1999; Wang, 2000) with a certain phase between the two motions. It would, therefore, be beneficial to gain the performance of dual actuation with only one input parameter actively imposed and the remaining actuation parameter passively determined by the properly designed system. In this study, we choose to actuate the pitch actively and let the plunge passively occur rather than the reverse situation because pitch is, generally, a simpler motion to create mechanically. Further, all of the simulations in this work use a simple harmonic pitch actuation, with an actuation amplitude of $\pm 15^\circ$.

We choose the normalized spring stiffness values of $K_n = 2.0,\ 20.0$, and 200.0 throughout this paper because they show the behavior of weak (2.0) intermediate (20.0) and strong (200.0) translational springs. The dynamics in the

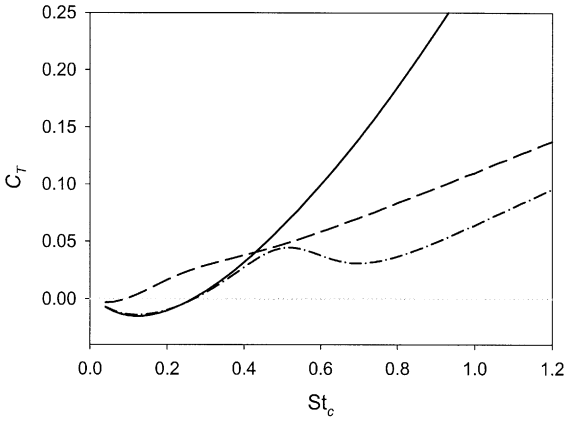

Fig. 3. Coefficient of thrust plotted against the Strouhal number for three values of normalized spring stiffness $K_n = 2.0$ (– – –), $K_n = 20.0$ (– · –), $K_n = 200.0$ (——). The weaker spring allows the propulsor to plunge in response to the instantaneous fluid forces placed on the propulsor. The resulting combination of pitch and passive plunge reduces the frequency for which positive thrust is produced. This gives the benefits of dual actuation (pitch and plunge) with single actuation (pitch only).

intermediate range can vary substantially but our focus in this paper is to show the effect of this parameter rather to present an exhaustive study of spring stiffness and resulting flap performance. We set the upper and lower values of spring stiffnesses where significant changes in dynamics cease to occur. For spring stiffness values of 200.0 and greater, the propulsor acts similar to a propulsor pinned at the quarter-chord (Murray, 1999). Because the dynamics of thrust and efficiency of spring stiffness values greater than 200.0 match the results obtained for a pinned rigid propulsor they are not analyzed. For values of spring stiffness less than 2.0 there is no significant change in the thrust coefficient or efficiency for normalized frequencies greater than 0.3, and only small differences in thrust coefficient for normalized frequencies less than 0.3. Significant changes in propulsor dynamics do occur between the stiffness values of 2.0 and 200.0 and, therefore, we shall include a representative value of stiffness in this range.

Fig. 3 compares the thrust coefficient, Eq. (18), for oscillating propulsors with the three translational spring stiffnesses we consider. A clear point shown in the figure is the change in critical frequency with spring stiffness. This point is shown as the root in Fig. 3. For frequencies below the critical, the flap actuation—active pitch and passive plunge—creates negative thrust or induced drag. The flap produces thrust for frequencies greater than the critical value. As we show in Fig. 3, the critical frequency approaches zero for small spring constants while for large spring constants, the critical frequency approaches the value 0.272; the value for pure pitching motion about the quarter-chord we calculated and compares favorably to the value of 0.289 obtained by using the equations formulated by Garrick (1937). The most important point to be distilled from Fig. 3 is the reduction in critical frequency by the addition of passive plunge. This point is more clearly shown in Fig. 4 in which we show the critical frequency as a function of normalized spring stiffness, K_n. This reduction in critical frequency together with increased efficiency that we discuss in the next section can make the single actuated pitch with passive plunge flap competitive with a dual actuated flap.

We should make two further points regarding Figs. 3 and 4. First, the figures shows that, after a Strouhal number of about 0.75, the thrust increases for all spring values. The thrust will, indeed, increase without bound for large Strouhal numbers. This is, of course, not the case for real fluids. It is rather an artifact of the inviscid flow model we use in this work combined with the Kutta condition that will break down for large frequencies (Katz and Weihs, 1981). The second point we should make is the fact that all curves show no thrust (no drag) for vanishing frequency. This is directly due to our neglect of viscosity. In a real fluid, the system will (i) have nonzero drag at zero Strouhal number, (ii) have decreasing thrust for large Strouhal numbers as a result of stall, and (iii) show an increase in the critical Strouhal number as extra thrust is needed to overcome the viscous contribution to drag (Jones et al., 1998).

3.2. Thrust efficiency

We next turn to the thrust efficiency of active pitch–passive plunge actuation. In order to compute the efficiency we use Eq. (15) which is simply the ratio of power output (power generated in producing thrust) to power input (power expended in moving the flap). While other definitions of efficiency have been used in the literature (see, for example Garrick (1937) and Lighthill (1970)) this is the most straightforward and most meaningful definition. Note that by this definition, we can have negative efficiency. This occurs when the either power in or power out is negative. For the

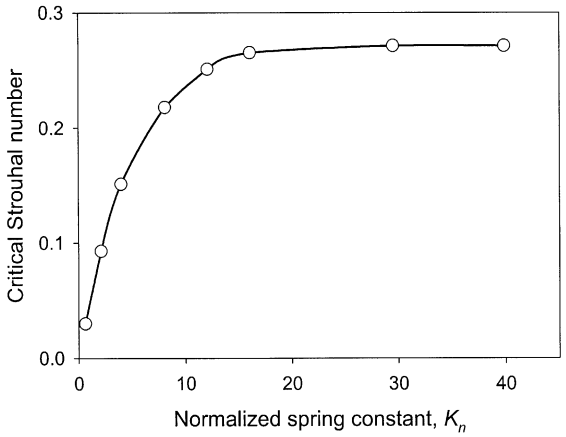

Fig. 4. Critical Strouhal number for thrust production plotted against normalized spring stiffness, K_n. For a given spring constant, actuation frequencies below the critical value result in induced drag. Note that for sufficiently stuff springs, the critical frequency is independent of spring constant.

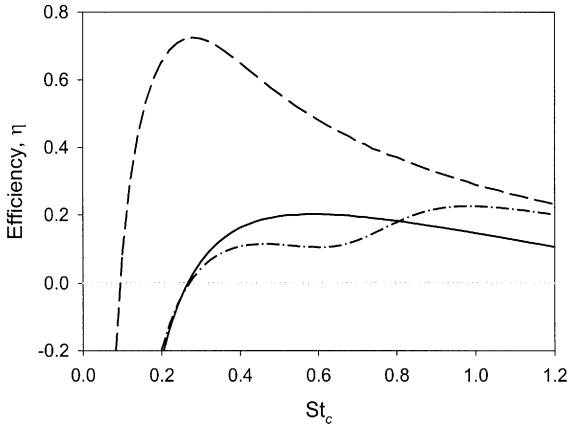

Fig. 5. Efficiency [see Eq. (15)] for a foil actuated in pitch with plunge determined passively by a translational spring. The efficiency of thrust production can be significantly increased by allowing the foil to plunge. The three curves correspond the normalized spring stiffness values $K_n = 2.0$ (– – –), $K_n = 20.0$ (– · –), $K_n = 200.0$ (——).

efficiency curves shown in Fig. 5 negative efficiency accompanies negative thrust (induced drag). None of the results shown in this paper have negative power input although we have considered these problems elsewhere (Murray, 1999).

Fig. 5 shows that, for sufficiently large Strouhal number, while the thrust may continue to increase with Strouhal number, the efficiency decreases. Most interesting is the maximum or peak efficiency for our three spring examples. The curve of large stiffness (200.0) is typical of actuation with little (or no) plunge. Peak efficiency for purely pitching actuation is typically approximately 0.2. For propellers, typical efficiencies are in the range of 0.65–0.75 or greater (Breslin and Andersen, 1994) depending on the loading. This makes thrust generation by pitch actuation alone prohibitively expensive when compared to highly efficient methods such as rotary propellers.

When both pitch and plunge motions are present, a significant increase in efficiency is possible over that case of pitch only. Our results show that the best efficiency values are associated with high plunge amplitudes (Fig. 6). The high efficiencies (> 80%) obtained by Anderson et al. (1998) were nominally associated with large plunging magnitudes combined with pitching. Many biological swimmers and fliers use a combination of pitching and plunging of their fins or wings (Azuma, 1992; Hall and Hall, 1996). Further, researchers using variational methods (Hall and Hall, 1996) and experimental techniques (Dickinson et al., 1999) find that the optimal flight actuation places most of the shed vorticity at the extremes of the wing trailing edge path. This is also the case in our work. For example, with a spring stiffness of 2.0 and a St_c between 0.2 and 0.4, the flap motion places the greatest amount of shed vorticity (with the appropriate rotational sense) near the top and bottom of the trailing edge flight-path.

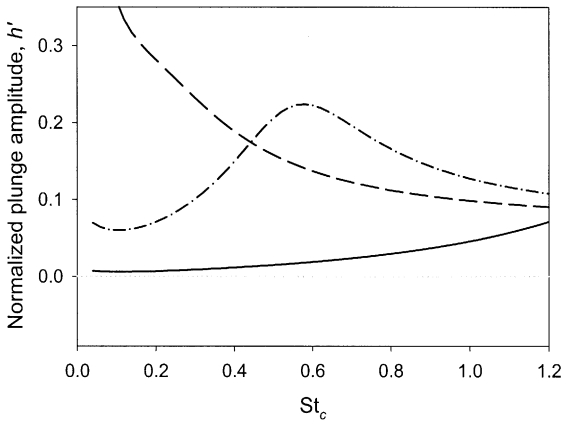

Fig. 6. Normalized plunge amplitude of the pivot point vs. Strouhal number for three values of normalized spring stiffness $K_n = 2.0$ (– – –), $K_n = 20.0$ (– · –), $K_n = 200.0$ (——). Weak (strong) springs produce displacement that decreases (increases) with increased frequency. Springs in the intermediate ranges—20.0 in this case—exhibit a damped resonance response with driving frequency. This resonance condition can result in a local minimum in thrust efficiency (see the corresponding curve in Fig. 5).

3.3. Heave amplitude and actuation phase

Fig. 6 shows the normalized plunge response, h', expressed as a fraction of the chord length, for the three spring values considered in this work. We define the plunge, at the quarter-chord pivot point, as the absolute maximum excursion of the pivot point from the unstrained configuration. Stiff and weak springs behave as one expects. The stiff translational spring restrains the displacement of the pivot point to small values for reasonable Strouhal numbers. For smaller values of normalized frequency, the plunge displacement is small because the hydrodynamic forces cannot cause significant spring deflection. At the higher frequencies the increased hydrodynamic forces are able to displace the propulsor. Conversely, the weak spring allows the pivot point to make large excursions from the rest configuration with the greatest excursions occurring for small Strouhal numbers. Here, the system deflection is dominated by the 'apparent mass' of the fluid. For the smaller driving frequencies, the response is large because system has more time to respond each period and the acceleration of the 'apparent mass' is small. As the frequency increases, the apparent mass effect also increases. This coupled with the smaller time for the foil to respond causes the displacement amplitude to decrease. In the intermediate region, displacement vs. frequency curves exhibit behaviors typical of damped oscillators. Although we add no damping explicitly to our model, it is nevertheless present in the form of aerodynamic damping for the unsteady system (Dowell, 1994). This effectively prevents divergent behavior at mechanical resonance.

The trailing edge amplitude response, Fig. 7, for the larger value of spring stiffness can be explained qualitatively utilizing the plunge response of the pivot together with the plunge phase, shown in Fig. 8. The plunge phase is defined as the phase difference between the pitch angle and the pivot plunge response. The trailing edge displacement is the combination of the plunge displacement and the displacement caused by the propulsor pitch.

The curve of trailing edge amplitude for the larger value of spring stiffness remains fairly constant. For the smaller values of normalized frequency the trailing edge amplitude is simply the displacement caused by the pitching of the propulsor, because the plunge magnitude is insignificant. For larger values of normalized frequency, the plunge phase approaches -90° and, therefore, the magnitude of the trailing edge increases only slightly by plunge. For the smaller value of spring stiffness, 2.0, the trailing edge displacement is primarily determined by the pivot plunge amplitude at lower frequencies. At large frequencies both pivot heave and angular displacement contribute. The intermediate value of spring stiffness of 20.0 demonstrates a resonance phenomenon, where the plunge amplitude reaches a relative maximum at a normalized frequency of approximately 0.6, and the trailing edge amplitude reaches a relative minimum at approximately the same value. Although the normalized frequency where the maximum plunge and trailing edge amplitudes occur are approximately equal for a spring stiffness of 20.0, this is generally not the case.

4. Conclusions

In summary, we developed a computational tool to analyze the dynamics of a pitching thin foil allowed to passively plunge. The computational model utilizes a vortex lattice method and calculates plunge implicitly. Thrust and efficiency

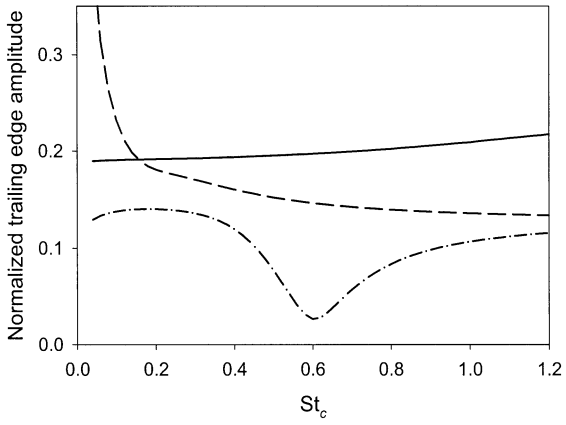

Fig. 7. Normalized trailing edge plunge amplitude vs. Strouhal number for three normalized spring stiffnesses $K_n = 2.0$ (– – –), $K_n = 20.0$ (– · –), $K_n = 200.0$ (——). Strong and weak springs produce plunge behavior similar to the pivot point plunge behavior shown in Fig. 6. The local minimum in trailing edge plunge for the intermediate value of spring constant corresponds to a local maximum on plunge amplitude for the pivot point.

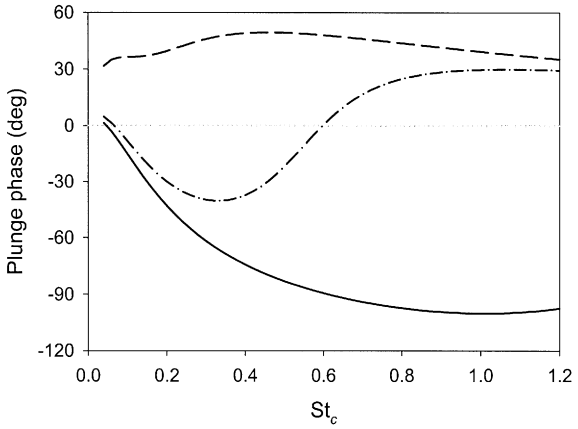

Fig. 8. Phase difference between the pitch angle and resulting plunge angle as a function of normalized frequency. Plunge angle generally leads pitch angle for weak springs, $K_n = 2.0$ (– – –), while plunge angle generally lags pitch angle for strong springs, $K_n = 200.0$ (——). Intermediate strength springs, $K_n = 20.0$ (– · –), can produce positive or negative phase angle depending on the frequency.

values are obtained through analysis of the wake and the momentum imparted to the fluid. The singularly actuated system, simulated in our computational model, utilizes the inherent benefits of more elaborately actuated systems. These benefits are gained by the addition of an implicitly determined degree of freedom. The system is an easily implemented engineering design consisting of a pitch actuated foil with a compliant drive shaft.

We demonstrated that the critical frequency for positive thrust production is reduced by allowing passive plunge. Garrick (1937) demonstrated analytically the thrust produced was dependent on not only the frequency of oscillation, but also the relative magnitude and phase of between the pitch and plunge. As plunging motion supplements the pitching, the frequency above which positive thrust occurs is decreased. Qualitative analysis of the vortex sheet is used to determine whether hydrodynamic forces produces thrust or drag. Koochesfahani (1989) and Jones et al. (1998) demonstrated that the maximum magnitude of thrust was produced at frequencies that shed vorticity concentrates at the extremes of the trailing edge path, and zero thrust when predominantly shed at the mean line. Our work has shown that the addition of plunge also shifts the location of shed vorticity toward the extremes of the trailing edge path.

We also demonstrated that a single actuated system can achieve efficiencies competitive with dual actuated systems. This simple single actuated system also takes advantage of the gains in efficiency associated with the combination of pitch and plunge without the associated mechanical complexity of multiple actuators. Triantafyllou and Triantafyllou

(1995) and Anderson et al. (1998) demonstrated experimentally that a complicated dual actuated foil can have high peak efficiencies for certain combinations of pitch, plunge, and actuation frequency. These peak efficiencies, as high as 87% occur at Strouhal numbers (St_a) less than 0.5. Hall and Hall (1996,2000) utilized a variational principle to determine the optimum circulation distribution in flapping flight. Hall reports efficiencies as high as 85% for constant speed flapping flight. Wang (2000) showed that a combination of pitching and plunging produced the maximum efficiencies for low Reynolds numbers. These peak efficiencies occurred at Strouhal numbers (St_c) less than 1.0. In this work we report efficiencies above 70% at a Strouhal number (St_c) of 0.25.

Propulsive foils utilizing pitching actuation are used for very specialized applications. Highly maneuverable underwater vehicles requiring maximum agility use pitch actuated thrusters to obtain maximum acceleration with minimal mechanical complexity (Hobson et al., 1999). These thrusters suffer from low cruising efficiency, but increases in efficiency can be achieved by utilizing passive plunge.

In future work we plan to further investigate more aspects associated with single actuated foils. We plan on expanding our model to include the effects of a finite aspect ratio and turbulent boundary layers. We also plan on analyzing the effect of shifting the center of rotation. Finally, we hope to construct a test apparatus to verify the results we obtain.

Acknowledgements

The authors would like to thank Kenneth Hall and John Rule for many helpful discussions. The authors would also like to acknowledge the support of Office of Naval Research through Grant N00014-99-1-0452.

References

Anderson, J.M., Kerrebrock, P.A., 1999. The vorticity control unmanned undersea vehicle (VCUUV) performance results. Proceedings of the 11th International Symposium Unmanned Untethered Submersible Technology, Durham, NH, pp. 360–369.

Anderson, J.M., Streitlein, K., Barrett, D.S., Triantafyllou, M.S., 1998. Oscillating foils of high propulsive efficiency. Journal of Fluid Mechanics 360, 41–72.

Ashley, H., Landahl, M., 1965. Aerodynamics of Wings and Bodies. Dover, New York.

Azuma, A., 1992. The Biokinetics of Flying and Swimming. Springer, Tokyo.

Breder, C.M., 1926. The locomotion of fishes. Zoologica 4, 159–297.

Breslin, J.P., Andersen, P., 1994. In: Dyer, I., Taylor, R.E., Newman, J.N., Price, W.G. (Eds.), Hydrodynamics of Ship Propellers. Cambridge University Press, Cambridge, UK.

Chopra, M.G., 1974. Hydromechanics of lunate-tail swimming propulsion. Journal of Fluid Mechanics 64, 375–391.

Chopra, M.G., 1976. Large amplitude lunate-tail theory of fish locomotion. Journal of Fluid Mechanics 74, 161–182.

Chopra, M.G., Kambe, T., 1977. Hydromechanics of lunate-tail swimming propulsion. Part 2. Journal of Fluid Mechanics 79, 49–69.

Delaurier, J.D., Harris, J.M., 1982. Experimental study of oscillating-wing propulsion. Journal Aircraft 19, 368–373.

Dickinson, M.H., Lehmann, F.-O., Sane, S.P., 1999. Wing rotation and the aerodynamics of insect flight. Science 284, 1954–1960.

Dowell, E.H. (Ed.), 1994. A Modern Course in Aeroelasticity, 3rd Edition. Kluwer Academic Publishers, Boston, MA.

Garrick, I.E., 1937. Propulsion of a flapping and oscillating airfoil. NACA Report No. 567, pp. 419–427.

Gray, J., 1936. Studies in animal locomotion. VI. The propulsive powers of the dolphin. Journal of Experimental Biology 13, 192–199.

Hall, K.C., Hall, S.R., 1996. Minimum induced power requirements for flapping flight. Journal of Fluid Mechanics 323, 285–315.

Hall, K.C., Hall, S.R., 2000. A rational engineering analysis of the efficiency of flapping flight. Presented at the Conference on Fixed, Flapping and Rotary Wing Vehicles at Very Low Reynolds Numbers, Notre Dame, IN.

Hall, K.C., Pigott, S.A., Hall, S.R., 1997. Power requirements for large amplitude flapping flight. AIAA 35th Aerospace Sciences Meeting & Exhibit, Reno, NV, pp. 1–11.

Harper, K.A., Berkemeier, M.D., Grace, S., 1998. Modeling the dynamics of spring-driven oscillating-foil propulsion. IEEE Journal of Ocean Engineering 23, 285–296.

Hobson, B., Pell, C., Murray, M.M., 1999. Pilotfish: Maximizing agility in an unmanned-underwater vehicle. Proceedings of the 11th International Symposium Unmanned Untethered Submersible Technology, Durham, NH, pp. 41–51.

Jones, K.D., Dohring, C.M., Platzer, M.F., 1998. Experimental and computational investigation of the Knoller-Betz effect. AIAA Journal 36, 1240–1246.

Katz, J., Plotkin, A., 2001. Low-Speed Aerodynamics, 2nd Edition. Cambridge University Press, Cambridge, UK.

Katz, J., Weihs, D., 1981. Wake rollup and the Kutta condition for airfoils oscillating at high frequency. AIAA Journal 19, 1604–1606.

Koochesfahani, M.M., 1989. Vortical patterns in the wake of an oscillating airfoil. AIAA Journal 27, 1200–1205.

Krasny, R., 1987. Computation of vortex sheet roll-up in the Trefftz plane. Journal of Fluid Mechanics 184, 123–155.

Kumph, J.M., Triantafyllou, M.S., Nugent, D., dos Santos, M., 1999. Fast starting and maneuvering vehicles: Robopike and robomuskie. Proceedings of the 11th International Symposium Unmanned Untethered Submersible Technology, Durham, NH, pp. 439–445.

Lighthill, M.J., 1960. Note on the swimming of slender fish. Journal of Fluid Mechanics 9, 307–317.

Lighthill, M.J., 1970. Aquatic animal propulsion of high hydrodynamical efficiency. Journal of Fluid Mechanics 44, 265–301.

Marey, E.J., 1874. Animal Mechanism: A Treatise on Terrestrial and Aerial Locomotion. H. S. King, London.

Murray, M.M., 1999. Hydroelasticity modeling of flexible propulsors. Ph.D. Dissertation, Duke University, Durham, NC.

Pettigrew, J.B., 1874. La locomotion chez les animaux. G. Baillière, Paris.

Saffman, P.G., 1967. The self-propulsion of a deformable body in a perfect fluid. Journal of Fluid Mechanics 28, 385–389.

Taylor, G., 1952. An efficient swimming machine. Proceedings of the Royal Society of London Series A: Mathematical and Physical Sciences 214, 158–183.

Theodorsen, T., 1935. Mechanism of flutter a theoretical and experimental investigation of the flutter problem. NACA Report No. 496, pp. 413–433.

Triantafyllou, M.S., Triantafyllou, G.S., 1995. An efficient swimming machine. Scientific American 272, 64–70.

Triantafyllou, G.S., Triantafyllou, M.S., Gopalkrishnan, R, 1991. Wake mechanics for thrust generation in oscillating foils. Physics Fluids A 3, 2835–2837.

Triantafyllou, G.S., Triantafyllou, M.S., Grosenbaugh, M.A., 1993. Optimal thrust development in oscillating foils with application to fish propulsion. Journal of Fluids Structures 7, 205–224.

von Kármán, T., Burgers, J.M., 1935. In: Durand, D.F. (Ed.), Aerodynamic Theory, Vol. II. Julius-Springer, Berlin.

Wang, Z.J., 2000. Vortex shedding and frequency selection in flapping flight. Journal of Fluid Mechanics 410, 323–341.

Wu, T.Y., 1961. Swimming of a waving plate. Journal of Fluid Mechanics 10, 321–344.